Morphologies and Properties of Nanocomposite Films Based on a Biodegradable Poly(ester)urethane Elastomer

Tae Woong Cho, Seong Woo Kim

Department of Chemical Engineering, Kyonggi University, 94-6 Yiui-Dong Yeongtong-Gu, Suwon, Gyeonggi-Do 443-760, South Korea

Received 29 May 2010; accepted 9 November 2010
DOI 10.1002/app.33766
Published online 4 March 2011 in Wiley Online Library (wileyonlinelibrary.com).

ABSTRACT: Biodegradable poly(ester)urethane (PU) elastomer-based nanocomposite films incorporated with organically modified nanoclay were prepared with melt-extrusion compounding followed by a casting film process. These films were intended for application as biodegradable food packaging films, with their enhanced gas barrier, mechanical, and thermal properties and good flexibility. From both X-ray diffraction measurements and transmission electron microscopy observations, the coexistence of intercalated tactoids and exfoliated silicate layers in the compounded PU/clay nanocomposite films was confirmed. In addition, the morphology exhibited a clay dispersion state in the matrix and was influenced by the incorporated nanoclay content. The effects of the nanoclay loading level on the thermal, mechanical, and barrier properties of the compounded nanocomposites were also investigated. As a result, it was revealed that the addition of nanoclay up to a certain level resulted in a remarkable improvement in the thermal properties in terms of thermal stability and the degree of thermal shrinkage; mechanical properties, including dynamic storage modulus and tensile modulus; and oxygen/water-vapor barrier properties of the nanocomposite films. © 2011 Wiley Periodicals, Inc. J Appl Polym Sci 121: 1622–1630, 2011

Key words: barrier; biomaterials; morphology; nanocomposites

INTRODUCTION

Packaging films produced from polymeric materials are widely used in the food industry as these plastic materials have many advantages, as they are lightweight, flexible, strong, transparent, and easy to process compared to metal and glass.[1–3] Food packaging films need to provide appropriate resistances to oxygen and water-vapor permeation and must possess adequate mechanical properties to safely maintain product quality during the storage and handling time period (commonly called *shelf life*).[4] In general, packaging films with high barrier and mechanical properties are usually produced with a multilayered structure with a variety of polymer resins, such as polyolefin, polyamide, poly(ethylene terephthalate), and ethylene/vinyl alcohol copolymer.[5]

However, these synthetic polymer materials obtained from petrochemicals are practically nondegradable; this can become a serious environmental problem after their useful life. From this point of view, intensive efforts to develop ecologically safe biodegradable polymer materials for the application of short-term storage packaging films are underway.[6] In recent years, conventional nondegradable polymer materials for use in the manufacturing of food packaging films have been replaced by environmentally friendly biodegradable polymer resins obtained from petrochemicals or renewable resources.[7,8] Unfortunately, packaging films produced with biodegradable materials have some drawbacks that severely limit their use in industrial applications, including poor barrier, mechanical, and thermal properties.[5]

Therefore, to overcome these shortcomings and to improve the properties of biodegradable polymers, many research attempts have been made to combine the polymers with other synthetic polymers or inorganic components.[7,9,10] In particular, great attention has been focused on organic–inorganic nanocomposite materials in which organically modified layered silicates are dispersed at the nanometer scale in a polymeric matrix. Such polymer nanocomposites exhibit greatly improved mechanical, thermal, barrier, and fire-retardant properties with very low clay contents compared to those of virgin polymers or conventional composites with micrometer scales.[11–13] It has been recognized that these remarkable improvements in the nanocomposite properties originate from the homogeneous dispersion of intercalated or exfoliated layered silicate platelets in the continuous polymer matrix and the high degree of interfacial attraction between the organic polymer molecules and the inorganic silicate phase.[14–16]

Correspondence to: S. W. Kim (wookim@kyonggi.ac.kr).

Accordingly, biodegradable polymers have been incorporated with layered silicates at a very high aspect ratio (10–1000) to produce biodegradable nanocomposites with enhanced properties. Many studies have been conducted on biodegradable nanocomposites based on aliphatic thermoplastic polyesters such as poly(lactic acid) (PLA),[17,18] poly(butylene succinate),[19,20] and poly(ε-caprolactone).[21] Among these biodegradable polymers, PLA synthesized from renewable resources has attracted much attention as it exhibits excellent mechanical properties, biodegradation properties, biocompatibility, and transparency in the processed films. Despite its many advantages, however, crystalline PLA has limitations for application as food wrapping films because of its high stiffness and poor heat distortion temperature.[22] Although PLA is reinforced by inorganic layered silicates with high rigidity, the resultant PLA-based nanocomposite still exhibits brittleness.

Therefore, in this study, the preparation of nanoclay-incorporated composites was attempted with a biodegradable thermoplastic polyurethane elastomer as a polymer matrix to enhance the mechanical, thermal, and barrier properties and to impart flexibility to the produced nanocomposite film, an essential property of food packaging films. Poly(ester)urethane (PU) elastomer based nanocomposite films incorporated with quaternary ammonium-modified montmorillonite [Cloisite 30B (C30B)] were prepared via a twin-extrusion compounding process followed by a single-extrusion casting film process. We investigated the platelet clay dispersion state in the matrix through transmission electron microscopy (TEM) observation and X-ray diffraction (XRD) analysis. We also examined the variations in the mechanical, thermal, rheological, and barrier properties of the prepared PU nanocomposites as a function of the clay content.

EXPERIMENTAL

Materials

A thermoplastic biodegradable PU elastomer was obtained from Sejeong C&M with grade name EN-805. The organically modified montmorillonite used in this study was purchased from Southern Clay Products (Gonzales, TX, USA) with the commercial name Cloisite 30B (C30B; cation-exchange capacity = 90 mequiv/100 g); it was modified with a quaternary ammonium slat containing one methyl, one tallow, and two hydroxyethyl groups.

Before melt-compounding processing, polyurethane in the form of pellets and clays were dried in a convective drying oven at 60°C for 24 h and in a vacuum oven at 80°C for 12 h, respectively, to remove moisture contained within the materials.

Preparation of the nanocomposite film

The melt compounding of PU with the clay particles was performed on a corotating intermeshing twin-screw extruder (ZSK25, Werner & Pfleiderer, Germany) with a screw diameter of 25 mm and a screw length to diameter ratio (L/D) of 40. It was operated at a screw rotation speed of 300 rpm and with a temperature profile between 180 and 190°C. The melt-extruded PU/clay nanocomposite strand emerging from the die was cooled in a water bath and then cut into cylinder-type pellets with a pelletizer. The compounded pellets were dried in a fluidized bed-type dryer (Buss Co.) before further processing, and then, the nanocomposite films with thicknesses ranging from about 60 to 70 μm were produced by a casting film process with a single-screw extruder attached to a T-die (D-5489, Plastik Paschinenbau Co., Germany).

When preparing the nanocomposites, the incorporated clay contents were varied at 3, 5, and 7 wt %, accordingly, and the samples were designated as PUCL3, PUCL5, and PUCL7, respectively.

Characterization

The molecular weights of the neat PU resin before compounding and PU resins in the compounded nanocomposites were measured with gel permeation chromatography (GPC; Viscotek GPC Max, Viscotek Co., Houston, TX, USA). The polyisobutylene standard for calibration and tetrahydrofuran as a carrier solvent were used in the GPC analyses. The nanoclay particles in the nanocomposite samples were removed with a microsyringe filter before they were injected into the GPC column.

The gallery distance in the clay intercalated by polyurethane molecules during melt compounding was quantitatively measured on an X-ray diffractometer (3D Max-C, Rigaku, Tokyo, Japan) with Cu Kα radiation operated at 40 kV and 30 mA. The samples were scanned in the range 1–10° at a scanning rate of 1.0°/min. The analysis of the compounded nanocomposites was carried out in the form of casting thin film, whereas the pristine clay was analyzed in the powder form. The basal spacing of the clay was determined from the position of the interlayer basal spacing (d_{001}) peak in the XRD pattern with Bragg's law.

The clay dispersion state in the nanocomposites was qualitatively observed with TEM (Tecnai G2, Fei, Hillsboro, OR, USA) at an accelerating voltage of 200 kV. The specimens, with a thickness of about 100 nm for TEM observation, were prepared by ultramicrotoming of the cured epoxies containing nanocomposite film with a diamond knife.

Thermogravimetric analysis (TGA) of the PU/clay nanocomposite was performed with a PerkinElmer TGA-7 instrument (Norwalk, CT, USA) at a heating rate of 10°C/min in the temperature range 25–800°C.

TABLE I
Basic Properties of the Neat PU and Melt-Compounded PUs with Various Clay Contents

Sample	MFI (g/10 min)[a]	Density (g/cm^3)	M_w (g/mol)	PDI
Neat PU	14.4	1.20	24,904	1.105
PUCL3	13.6	1.22	19,377	1.300
PUCL5	12.5	1.23	19,237	1.319
PUCL7	10.3	1.23	19,875	1.392

[a] Measured at 190°C under a 2.16-kg loading (ASTM D 1238).

In addition, the thermal stability of the nanocomposite was also evaluated by the measurement of the thermal shrinkage for the nanocomposite films; this measurement was based on the method from ASTM D 2732. The pure PU film and corresponding nanocomposite films with various clay contents were thermally treated at different temperatures (80, 100, and 120°C) for 1 h, and then, the degree of thermal shrinkage was determined from the following equation:

$$\text{Shrinkage}(\%) = [(L_0 - L_f)/L_0] \times 100\% \quad (1)$$

where L_0 and L_f are the dimensions of the initial film and contracted film before and after thermal treatment, respectively.

The dynamic viscoelastic properties of the nanocomposite materials were measured with a dynamic mechanical analyzer (Seiko Exter SS6100, Seiko Co., Yokyo, Japan) with a strain amplitude of 0.1% at a frequency of 1 Hz. The temperature was increased from −50 to 120°C at a heating rate of 2°C/min.

Tensile tests for the nanocomposite films prepared by the extrusion casting film process were performed according to ASTM D 638 with a universal testing machine (QM100S, Qmesys, Sungnam, Korea) at a cross speed of 50 mm/min. Five samples with dimensions of 10 mm (width) × 70 mm (length), which were taken in the machine direction (MD) and the transverse direction (TD), were tested in each case, and an average value was taken.

The oxygen permeability of the nanocomposite casting film was measured by a handmade permeation apparatus, which was designed and made according to the standard method of ASTM D 3985. Detailed descriptions of the apparatus and experimental measurements were given elsewhere.[23,24] The water-vapor transmission rate was measured with a MOCON instrument (Permatran-W 3/33, Minneapolis, MN, USA), and the test method was based on ASTM F1249.

RESULTS AND DISCUSSION

Basic properties

Basic properties, including the molecular weight, density, melt flow index (MFI), and polydispersity index (PDI), of the neat PU and melt-compounded PUs with various organoclay contents are shown in Table I. The weight-average molecular weight (M_w) of the PU decreased by 22–27% depending on the clay content in the melt-compounded nanocomposites. This reduction in the PU molecular weight was attributable to not only physical degradation caused by the high shear stress and temperature generated within the twin-screw extruder but also to chemical degradation by the reaction of C30B surfactant degradation products with isocyanates from the urethane during the high-temperature melt-compounding process.[25] The formation of low-molecular-weight PU molecules induced by these degradation mechanisms should have given rise to an increase in PDI, which is a measure of the breadth of the molecular weight distribution. MFI of the melt-compounded PU, an estimate of the melt flow behavior, decreased despite the reduction in the melt viscosity because of the decreased molecular weight. Moreover, a significant decrease in MFI occurred as the amount of organoclay added to the nanocomposites increased. This result could be explained by the fact that the increased resistance to melt flow, which is typically observed in suspension systems incorporated with inorganic particles, dominated the reduction in the melt viscosity because of the degradation of polymer molecules.

Nanocomposite structure

In general, obtaining a homogeneous and uniform dispersion structure of intercalated or exfoliated silicate platelets in the polymer matrix has been considered as the key factor required for obtaining high-performance polymer nanocomposites.[12] In this study, the nanocomposite structure was examined with XRD analysis and TEM observation as quantitative and qualitative methods, respectively. Figure 1

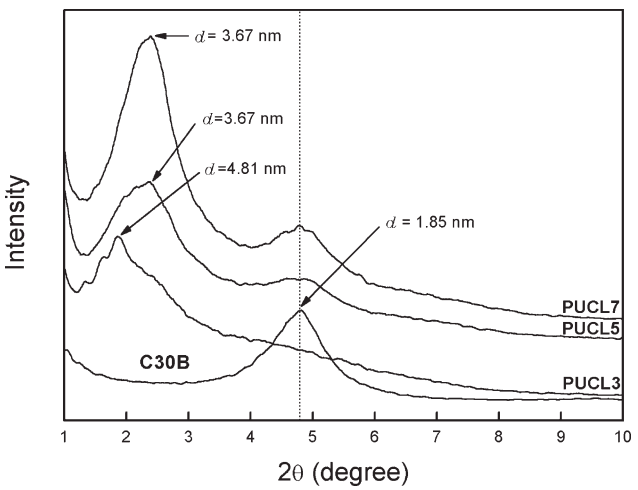

Figure 1 XRD patterns of pristine C30B and PU/clay nanocomposites with various clay contents.

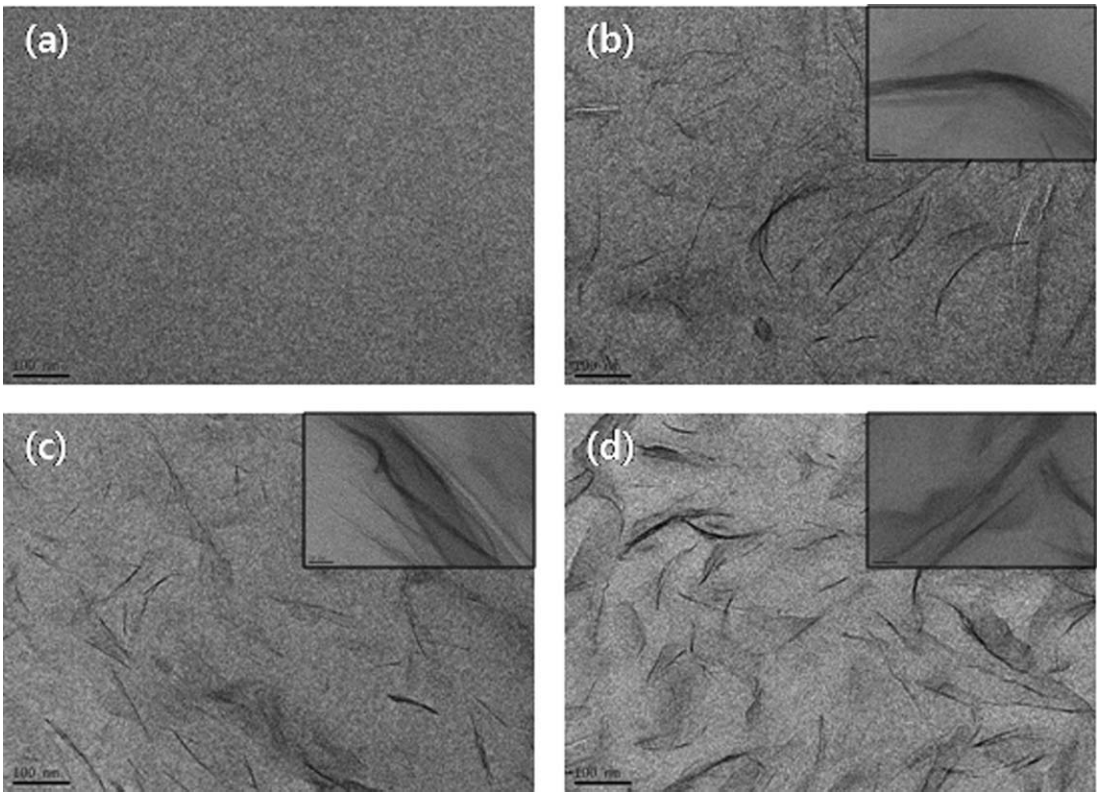

Figure 2 TEM images of neat PU and PU/clay nanocomposites with various clay contents: (a) neat PU, (b) PUCL3, (c) PUCL5, and (d) PUCL7.

shows the XRD patterns of the pristine C30B and corresponding nanocomposites with various clay loadings in the 2θ range 1–10°. The diffraction peak of the C30B clay exhibited at $2\theta = 4.8°$, which corresponded to a d_{001} of 1.85 nm, shifted to a lower 2θ value and corresponding larger d_{001} after nanocomposite preparation; this indicated the formation of an intercalated structure. The intercalated spacing between the clay platelets varied depending on the clay content in the nanocomposite. For example, the diffraction peaks appeared at $2\theta = 1.86°$ (d-spacing = 4.81 nm) in the case of 3 wt % clay loading and at $2\theta = 2.38°$ (d-spacing = 3.66 nm) in the nanocomposites with 5 and 7 wt % clay loadings. This result suggests that the incorporated clay content is a significant parameter affecting the intercalation process of polymer chains into the interlayer spacing between the clay platelets. A higher extent of intercalation was obtained in the nanocomposites with low clay loadings. The addition of clay with small amounts of 3 wt % induced a fully intercalated structure, whereas additions of 5 and 7 wt % clay caused partially intercalated structures and, at the same time, exhibited the original status of the clay; this was confirmed from the weak peak at about 4.8°, which corresponded to the diffraction peak of the pristine clay. Furthermore, the nanocomposite with 7 wt % clay content appeared to have a larger fraction of clay in its original status compared to the 5 wt % clay added sample; this may have been due to the more prominent peak. In addition, the intensities of the shifted diffraction peaks for the clay in the nanocomposites decreased as the clay content decreased from 7 to 3 wt %; this indicated that the number of stacked layers in the intercalated silicate tactoids resulting from the melt compounding process was reduced because of the additional exfoliation process. In particular, lower clay loadings resulted in a higher degree of exfoliation in the nanocomposites because of the greater effective shear stress transfer to the clay agglomerates.

The morphology of the clay dispersed and distributed in the PU matrix domain was qualitatively observed by TEM. Figure 2 shows TEM images of the PU and nanocomposites with various clay contents. Compared to the image of pure PU in Figure 2(a), the images in Figure 2(b–d) show dark areas of stacked clay C30B tactoids layers and bright fields corresponding to the PU matrix. From both the 100-nm-scale and the 20-nm-scale images (inset), one can see that the stacked silicate layers were well dispersed throughout the PU matrix and that the intercalated and exfoliated structures coexisted in all of the nanocomposite samples fabricated in this study. The results obtained from TEM observation in conjunction with the XRD analysis results show that

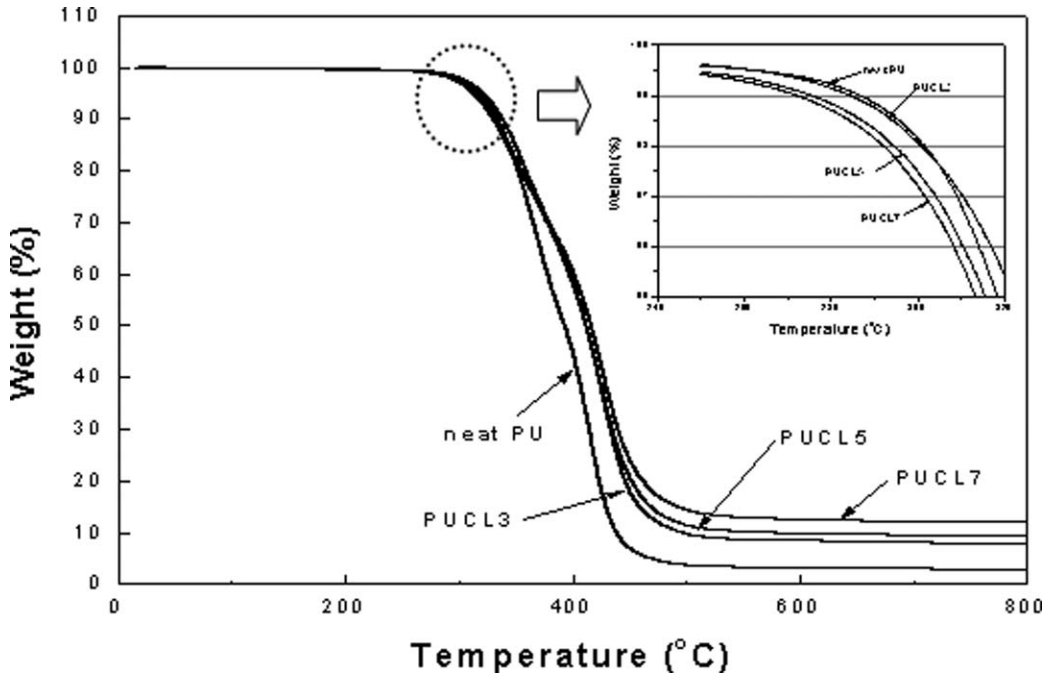

Figure 3 TGA thermograms of neat PU and PU/clay nanocomposites with various clay contents.

melt compounding with a twin-screw extruder was an effective process for the generation of intercalation and exfoliation of PU molecules into the clay C30B platelets because of its capability of providing high shear stress during processing. In addition, the C30B used in this study was an organically modified clay suitable for the preparation of biodegradable PU-based nanocomposites, as reported in previous studies, in which a good degree of intercalation or exfoliation could be achieved because of the strong hydrogen bonding between the carbonyl groups in the thermoplastic PU and the hydroxyl groups on the surface of the C30B clay platelets.[11,26] However, in the case of the nanocomposite with a 7 wt % clay loading, a somewhat poor dispersion of silicate layers was observed. In this sample, intercalated clay tactoids with a larger domain size were not uniformly distributed throughout the PU matrix, and it displayed a flocculated structure.

Thermal properties

In general, inorganic fillers with superior heat resistance have been used to improve the thermal stabilities of organic polymers. Hence, in this study, the thermal stabilities of biodegradable polyurethane nanocomposite films incorporated with small amounts of inorganic clay were evaluated with both TGA and thermal shrinkage measurements. Figure 3 shows the thermograms obtained from TGA of the PU/clay nanocomposites with different clay loadings. The thermal stability parameters, the degradation temperatures at 2 and 50% weight loss (T_2 and T_{50}, respectively), were obtained from the thermograms and are listed in Table II. T_2 decreased with increasing clay loading. In the initial period of heating, the added organoclay seemed to deteriorate the thermal stability of the nanocomposite because the weight loss in the initial heating step up to about 300°C occurred mainly because of volatilization resulting from the degradation of small surfactant molecules adsorbed onto the clay surface. However, in the higher temperature region above around 350°C, after the elimination of organic modifier from the clay, the trend of the degradation temperature variation with clay content in the nanocomposite was opposite that exhibited in the initial degradation step. As shown in Table II, T_{50} increased substantially by about 19°C upon addition of 3 wt % clay, as compared with that of the pure PU resin. However, with more than 3 wt % clay, the additional presence of inorganic clay in the nanocomposite had only a minor effect on increasing the degradation temperature of the PU/clay nanocomposites. Therefore, the thermal stability improved up to an

TABLE II
TGA Results for the Neat PU and PU/Clay Nanocomposites with Various Clay Contents

Sample	T_2 (°C)	T_{50} (°C)
Neat PU	301.4	393.1
PUCL3	300.6	412
PUCL5	294.3	412.2
PUCL7	292	416.5

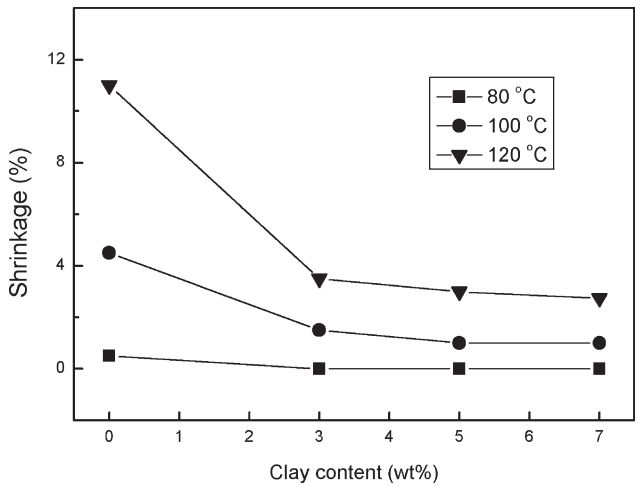

Figure 4 Thermal shrinkage percentage as a function of the clay content for neat PU and PU/clay nanocomposite films treated at different temperatures.

optimum level of clay content because of the efficient thermal barrier effect of clay platelets that were largely exfoliated in the PU matrix. However, with excess clay content beyond the optimum value, the contribution of inclusion clays to the enhancement of thermal stability became insignificant because of the low degree of exfoliation and poor dispersion, as confirmed in the previous TEM observation.

It is known that polymeric materials usually experience thermal shrinkage due to density changes when they are cooled from a soft rubbery or melt state with high chain mobility to a frozen solid state with restricted molecules. In particular, this phenomenon has been observed to be remarkable in thermoplastic crystalline polymers because a crystalline phase undergoes a much higher density change than does an amorphous phase during the solidification process. In the case of food packaging thermoplastic films (retort films or laminated films inside noodle containers for example), severe thermal shrinkage may occur when they are exposed to high-temperature boiling water. Hence, to minimize the degree of thermal shrinkage in the thermoplastic films, the incorporation of inorganic particles with high heat resistance is required for stable use as food packaging films.

In this study, the effect of added nanoclay on the thermal stability on the basis of the thermal shrinkage of the biodegradable PU/clay nanocomposite films was investigated. Figure 4 displays the thermal shrinkage percentages as a function of the clay content for the nanocomposite films treated thermally at various temperatures. At a low temperature of 80°C, the neat PU film exhibited a very low degree of shrinkage (0.5%), and incorporation of clay into the neat PU resin resulted in no thermal shrinkage (0%). On the other hand, at higher temperatures of 100 and 120°C, the neat PU films showed high degrees of shrinkage, 4.5 and 11.0%, respectively. The addition of only a small amount of clay (3 wt %) resulted in a remarkable reduction in the degree of thermal shrinkage, with thermal shrinkages of 1.5 and 3.5% at 100 and 120°C, respectively. Beyond a clay content of 3 wt %, however, the improvement in thermal stability based on thermal shrinkage was negligible, as shown in the figure. This trend of the variation of the thermal shrinkage with clay content was similar to that of the thermal degradation obtained from TGA measurements.

Dynamic viscoelastic properties

Dynamic mechanical analysis (DMA) was performed to examine the effects of clay incorporation into the PU resin on the viscoelastic properties as a function of temperature for the nanocomposites. Figure 5 shows the temperature dependences of the storage modulus corresponding to the elastic response to deformation for the neat PU and PU/clay nanocomposites over the temperature range −50 to 100°C. All of the nanocomposite samples incorporated with clay exhibited much higher storage moduli than those of neat PU over the entire investigated temperature region. This result was attributable to the mechanical reinforcement effect by the incorporation of inorganic nanoclay into the polymeric resin; this has usually been observed in organic–inorganic hybrid materials prepared at both the microscale and nanoscale levels. There was a prominent enhancement of the storage modulus by the incorporation of only a small amount of clay (3 wt %) as compared to that of neat PU. In addition, the storage

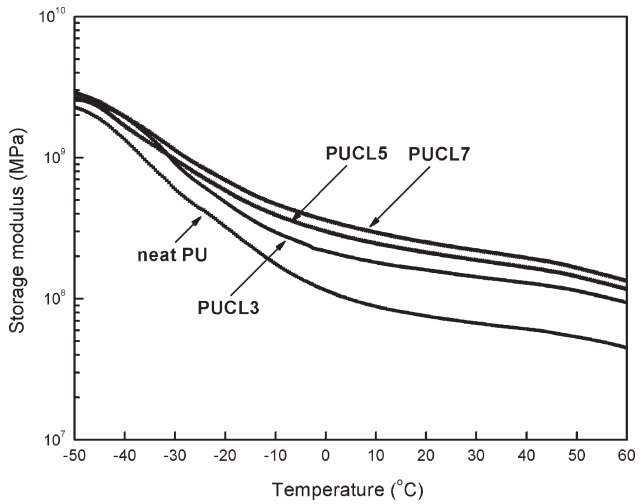

Figure 5 Dynamic storage modulus as a function of temperature for neat PU and PU/clay nanocomposites with various clay contents.

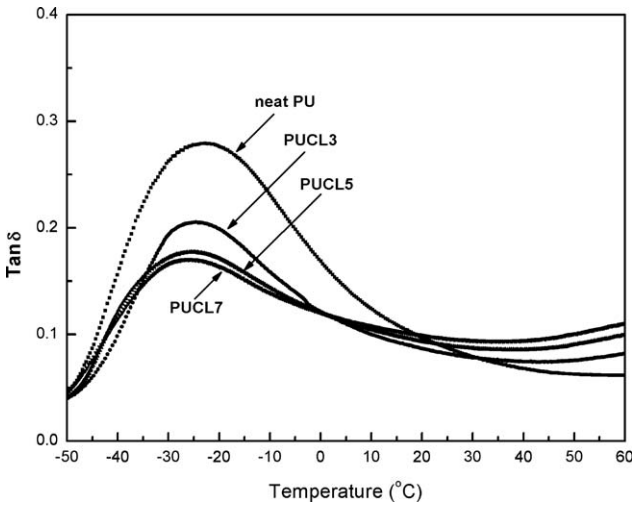

Figure 6 Tan δ as a function of temperature for neat PU and PU/clay nanocomposites with various clay contents.

moduli of the nanocomposites containing clay at levels of more than 3 wt % increased slightly with increasing clay loading level at temperatures below 60°C. Moreover, all of the nanocomposites exhibited roughly identical values of the storage modulus, regardless of clay content, in the rubbery plateau region above 60°C. Interestingly, this trend in the variation of the elastic properties with incorporated clay content in the nanocomposites, which was obtained from the DMA, was somewhat similar to that observed in the thermal property analysis presented in the prior section. In general, tan δ, (E''/E' ratio; E': storage modulus, E'': loss modulus) obtained from DMA, was used to determine the glass-transition temperature responsible for the polymer chain mobility transition occurring in the amorphous region. Figure 6 shows the temperature dependences of tan δ for the neat PU and nanocomposites containing various clay contents in the temperature range −50 to 100°C. The incorporation of clay did not cause a significant shift in the peak temperature in the tan δ curves toward higher temperatures. This behavior indicated that the interfacial attractions between the inorganic clay and organic PU phases in the intercalated nanocomposites, which originated from the hydrogen bonding formed between hydroxyl groups present on the surface of C30B and carbonyl groups in the PU molecules, was not strong enough to restrict the motions of amorphous chain segments located in the region adjacent to the interface.

Tensile properties

In the preparation of nanocomposite films with a casting film extrusion process, the PU molecules in the melt state or dispersed clay platelets were more highly oriented in the MD than in the TD because of the stretching operation caused by the difference between the take-up velocity of the rotating chilled roll and the velocity of the melt emerging from the T-die. Consequently, the produced nanocomposite films should have exhibited direction-dependent mechanical properties because of this orientation effect. Therefore, in this study, we investigated the tensile properties of the nanocomposite films in both the MD and TD. Figure 7 presents the tensile properties of the neat PU and the corresponding nanocomposite films measured in both the MD and TD. As observed in the storage modulus results obtained from DMA, the tensile moduli measured in both directions were considerably improved with increasing clay content up to 5 wt %. Beyond a clay content of 5 wt %, however, there was only a slight increase in the tensile modulus; this may have been due to the poor clay dispersion in the nanocomposites with an excess amount of clay, as observed in the TEM images. As the clay content increased, the tensile modulus in the MD increased more rapidly than that in the TD. That is, the increase in the amount of incorporated clay led to a larger discrepancy between the tensile modulus values in the MD and TD. This may have been a consequence of the orientation of nanoclay platelets along with the PU molecules, which occurred mainly in the extensional melt flow region between the T-die and the chilled roll. On the other hand, the elongation at break results of the nanocomposite films showed a marked contrast compared to the tensile modulus results. For neat PU, the elongation at break of the TD was much higher than that of the MD, and the discrepancy between the elongations measured in both directions became smaller with increasing clay content as a result of the opposite trend of elongation in each direction. In the nanocomposite system, an increase in the amount of inorganic clay with a very high stiffness generally gave rise to enhancements in the tensile modulus exhibiting the degree of stiffness but caused a reduction in the tensile elongation related to the flexibility. In the tensile property results, however, the elongation in the MD increased up to a 5 wt % clay content because of a rising effect resulting from the orientation of the clay platelets, which may have dominated reducing effect induced by the addition of the clay. Beyond a 5 wt % clay content, the elongations in both directions were reduced because of poor clay dispersion, as confirmed by the TEM observations. Meanwhile, the tensile strengths at break of the nanocomposite films in both directions were reduced with increasing clay content. This result was ascribed to the decrease in the molecular weight of PU caused by the degradation of the surfactant present on the C30B clay surface, as reported by Finnigan et al.[25]

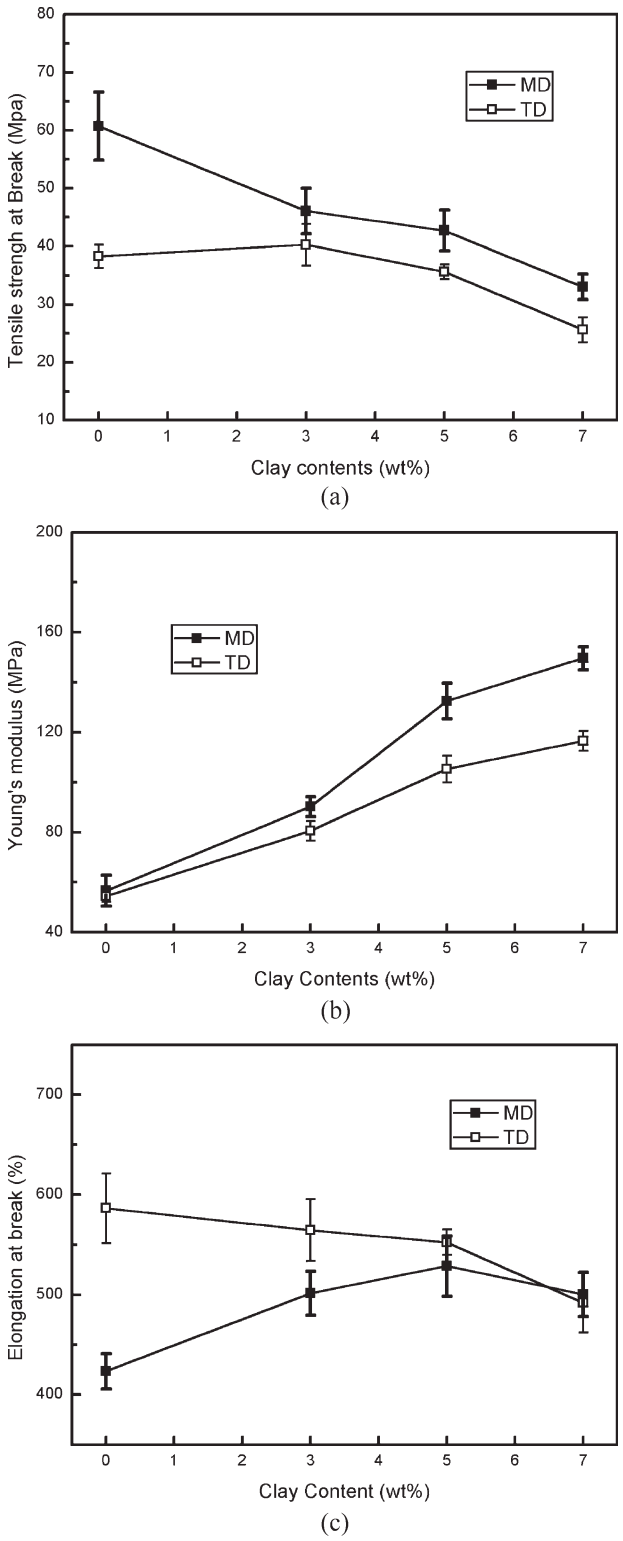

Figure 7 Tensile properties measured in both MD and TD as a function of the clay content for PU/clay nanocomposite films: (a) tensile strength at break, (b) Young's modulus, and (c) elongation at break.

Barrier properties

Much research involving polyolefin-based blend films with improved gas barrier properties have been performed by the incorporation of a small amount of high barrier polymer, such as ethylene/vinyl alcohol copolymer or polyamide.[1,2,27,28] Improvement of the gas barrier properties of these polymer blend systems has been achieved by the yielding of a lamellar structure with a high aspect ratio due to the stretching effect during the extrusion film process and by the dispersion of the high barrier polymer uniformly in the polyolefin matrix, which ultimately resulted in an increased tortuous path for penetrating gases. Accordingly, the incorporation of an inorganic layered silicate with a high aspect ratio is also expected to result in an improvement in the gas barrier properties by an increase in the tortuous path for penetrating gases. The gas permeation rate determined by the tortuous path in a nanocomposite is largely dependent on the extent of intercalation and exfoliation in the dispersed nanoclays. The oxygen and water-vapor permeabilities for the neat PU and corresponding nanocomposite films with various clay contents are presented in Figure 8. The oxygen permeability was dramatically decreased by 53% from 522.3 to 246.3 cc m^{-2} day^{-1} atm^{-1} by the addition of only a small amount of clay (3 wt %). However, only a slight decrease in the permeability was observed with increasing clay content above 3 wt %. On the other hand, the water-vapor permeability decreased considerably by 82% up to a 5 wt % clay loading. The water-vapor permeability decreased from 389.8 g m^{-2}·atm^{-1} (neat PU) to 242.4 g m^{-2}·atm^{-1} at a 3 wt % clay loading and to 67.92 g m^{-2}·atm^{-1} at a 5 wt % clay loading. However, an increased water-vapor permeability of 185.1 g m^{-2}·atm^{-1} was observed in the nanocomposite film containing 7 wt % clay; this may have been due to the poor clay dispersion with an excess amount of clay. On the basis of the oxygen and water-vapor permeability results, the improvement

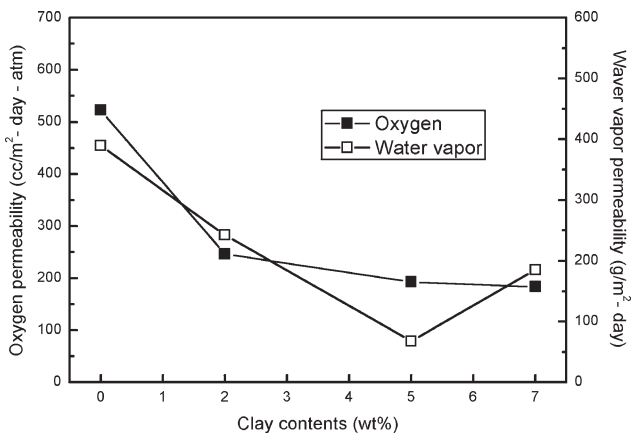

Figure 8 Oxygen and water-vapor permeability of neat PU and PU/clay nanocomposite films with various clay contents.

in the barrier properties was not observed when the incorporated nanoclay content was increased from 5 to 7 wt %. Moreover, in the water-vapor permeation, poor barrier properties were obtained with addition of a larger amount of nanoclay (7 wt %). Conclusively, when clay at a relatively high amount of 7 wt % was incorporated, a poor clay dispersion was observed; this resulted in poor water-vapor barrier properties, and no evident improvement was observed in the thermal, mechanical (modulus), or oxygen barrier properties. The incorporation of nanoclay at 5 wt % resulted in remarkable enhancements in the morphology and the performance of the prepared nanocomposite films. Accordingly, the amount of 5 wt % was an optimum level of clay content in the overall consideration of both the performance of the nanocomposite films and nanoclay cost.

CONCLUSIONS

Biodegradable PU elastomer based nanocomposite films containing organically modified nanoclay (C30B) were prepared with a twin-extrusion compounding process followed by a single-extrusion casting film process. The extents of intercalation and exfoliation of the clay platelets in the compounded nanocomposites were quantitatively evaluated in terms of the diffraction peak variation in the XRD measurements. The morphologies of the films were also qualitatively examined with TEM observations to evaluate the dispersion state of the clay. Despite the reduction of the PU molecular weight in the nanocomposites, which was caused by high shear stress, high temperature, and degradation products of surfactant present on the clay during the compounding process, the thermal stability; mechanical properties, including storage modulus and tensile modulus; and oxygen/water-vapor barrier properties of the produced nanocomposite films containing clay were enhanced in comparison with those of neat PU. These improvements were due to the simultaneously developed intercalation and exfoliation structures along with the well-dispersed silicate layers. In particular, the degree of thermal shrinkage was dramatically reduced upon the addition of only a small amount of nanoclay; this demonstrated the possibility for application to food packaging films such as retort films or laminated films inside noodle containers. In terms of the influence of clay content on the nanocomposite properties, a considerable enhancement was observed up to an optimum level of incorporated clay content. However, above a certain level of clay (5 wt %), a slight increase or reduction (in the case of water-vapor barrier properties) in the properties was observed because of poor clay dispersion.

References

1. Lohfink, G. W.; Kamal, M. R. Polym Eng Sci 1993, 33, 1404.
2. Faisant, J. B.; Kadi, A. A.; Bousmina, M.; Deschenes, L. Polymer 1998, 39, 533.
3. Samios, C. K.; Kalfoglou, N. K. Polymer 1998, 39, 3863.
4. Rhim, J. Food Sci Biotechnol 2007, 16, 691.
5. Blackwell, A. L. In Plastic Film Technology: High Barrier Plastic Films for Packaging; Finlayson, K. M., Ed.; Technomic: Lancaster, PA, 1989; p 41.
6. Lilichenko, N.; Marksimov, R. D.; Zicans, J.; Meri, R. M.; Plume, E. Mech Compos Mater 2008, 44, 45.
7. Sorrentino, A.; Gorrasi, G.; Vittoria, V. Trends Food Sci Technol 2007, 18, 84.
8. Tharanathan, R. N. Trends Food Sci Technol 2003, 14, 71.
9. Guilbert, S.; Cuq, B.; Gontard, N. Food Additives Contaminants 1997, 14, 741.
10. Petersen, K.; Nielsen, P. V.; Bertelsen, G.; Lawther, M.; Olsen, M. B.; Nilssonk, N. H. Trends Food Sci Technol 1999, 10, 52.
11. Dan, C. H.; Lee, M. H.; Kim, Y. D.; Min, B. H.; Kim, J. H. Polymer 2006, 47, 6718.
12. Chavarria, F.; Paul, D. R. Polymer 2006, 47, 7760.
13. Ma, X.; Lu, H.; Liang, G.; Yan, H. J Appl Polym Sci 2004, 93, 608.
14. Lee, S. K.; Seong, D. G.; Youn, J. R. Fibers Polym 2005, 6, 289.
15. Chen, G.; Yoon, J. Polym Degrad Stab 2005, 88, 206.
16. Krikorian, V.; Pochan, D. J. Chem Mater 2003, 15, 4317.
17. Ray, S. S.; Yanada, K.; Okamato, M.; Ueda, K. J Nanosci Nanotechnol 2003, 3, 503.
18. Chang, J.; An, Y. U.; Sur, G. S. J Polym Sci Part B: Polym Phys 2002, 41, 94.
19. Ray, S. S.; Okamato, K.; Okamato, M. J Appl Polym Sci 2006, 102, 777.
20. Shih, Y. F.; Wang, T. Y.; Jeng, R. J.; Wu, J. Y.; Teng, C. C. J Polym Environ 2007, 15, 151.
21. Yang, K.; Wang, X.; Wang, Y. J Ind Eng Chem 2007, 13, 485.
22. Li, Y.; Shimizu, H. Macromol Biosci 2007, 7, 921.
23. Yeo, J. H.; Lee, C. H.; Park, C. S.; Lee, K. J.; Nam, J. D.; Kim, S. W. Adv Polym Technol 2001, 20, 191.
24. Kim, D. J.; Kim, S. W. Korean J Chem Eng 2003, 20, 776.
25. Finnigan, B.; Martin, D.; Halley, P.; Truss, R.; Campbell, K. Polymer 2004, 45, 2249.
26. Meng, X.; Du, X.; Wang, Z.; Bi, W.; Tang, T. Compos Sci Technol 2008, 68, 1815.
27. Kim, S. W.; Chun, Y. H. Korean J Chem Eng 1999, 16, 511.
28. Holsti-Meittinen, R. M.; Perttila, K. P.; Seppala, J. V.; Heino, M. T. J Appl Polym Sci 1995, 58, 1551.